The electrospinnability of visco-elastic sugar solutions

Pablo G. T. Lepe[1], Nick Tucker[2], Andrew J. A. Watson[3], Deborah LeCorre-Bordes[4], Antony J. Fairbanks[3, 5], Mark P. Staiger[1]*

[1] Department of Mechanical Engineering, University of Canterbury, Private Bag 4800, Christchurch 8140, New Zealand.

[2] University of Lincoln, School of Engineering, Brayford Pool, LN6 7TS, Lincoln, United Kingdom.

[3] Department of Chemistry, University of Canterbury, Private Bag 4800, Christchurch 8140, New Zealand.

[4] The New Zealand Institute for Plant & Food Research Limited, Canterbury Agriculture & Science Centre, Gerald St, Lincoln 7608, New Zealand.

[5] Biomolecular Interaction Centre, University of Canterbury, Private Bag 4800, Christchurch 8140, New Zealand.

*Corresponding author: M. P. Staiger, Tel: (+64) (3) 364 2987, Fax: (+64) (3) 364 2078, E-mail: mark.staiger@canterbury.ac.nz

Abstract

It has been proposed that hydrogen bonding plays a role in promoting the electrospinnability of some materials. In this work, the significance of non-covalent interactions in the electrospinnability of aqueous sugar solutions (*i.e.* mono- and disaccharide) was investigated as a function of carbohydrate concentration. The electrospinnability of concentrated aqueous solutions of glucose, fructose and sucrose was studied by physicochemical and rheological characterization methods, and by subsequently examining the resulting morphology *via* scanning electron microscopy. The results on the electrospinning of concentrated saccharide solutions indicated the significance of non-covalent interactions on the electrospinning of these systems. Electrospinnability models based on critical concentration and visco-elasto capillary theories were compared with the experimental results. It is shown that visco-elasto capillary theory has the closest correlation with the experimental data. The electrospinnability of highly concentrated saccharide solutions appears to be directly related to the density and intermolecular bonding capacity of the solution.

Keywords: electrospinning, nanofibres, saccharide, hydrogen bonding, carbohydrates.

1. Introduction

Electrospinning is a method for the production of continuous polymer fibres with diameters in the sub-micron range [1-3]. During the electrospinning process, a high voltage is applied to a droplet of a polymer solution (or melt), stretching the droplet into a conical shape (known as the Taylor cone) by means of electrostatic repulsion [4]. A jet of polymer solution is emitted from the tip of the Taylor cone if the build-up of internal electrical charge overcomes the surface tension of the droplet. Given an appropriate combination of electro-viscoelastic properties, the polymer jet initially follows a stable, linear trajectory that resists the Plateau-Rayleigh instability, enabling it to be drawn into a fibre. Following stable jet formation, the jet typically undergoes a chaotic bending instability that leads to extensive jet thinning through solvent loss. A solid polymer fibre is then collected at an earthed electrode if sufficient solvent has been evaporated during the flight from tip to collector [1, 3, 5]. The ability of a polymer solution to resist the Plateau-Rayleigh instability during flight is usually attributed to the entanglement of polymeric molecules, and chain entanglement is commonly proposed to be the leading mechanism of fibre formation during electrospinning of polymeric systems [6, 7]. The formation of uniform electrospun polymeric fibres is thought to rely on the presence of at least 2 entanglements per chain [8, 9], although this may vary with polymer and its polydispersity and/or degree of branching [10]. However, some polymers may transition from electrospraying to electrospinning (as evidenced by the formation of beads-on-a-string) at concentrations between the critical overlap concentration (c^*) (*i.e.* semi-dilute, un-entangled) and the entanglement concentration (*Ce*) (*i.e.* semi-dilute, entangled), where *Ce* is typically ~$10 \times c^*$ [6, 54].

An alternative approach used to describe the concept of electrospinnability is the visco-elasto capillary theory [11-14]. According to visco-elasto-capillary thinning theory, non-Newtonian

fluids that undergo shear thinning and where $G' > G''$ at higher angular frequencies are able to better resist extensional capillary thinning and filament break-up when compared with Newtonian fluids for which $G' < G''$ at lower angular frequencies. Also, fluid inertia, as evidence by beads-on-string morphology, is also an important factor on the development of capillary waves. According to the visco-elasto-capillary theory, when the inverse of the fluid's relaxation time exceeds the rate of capillary thinning (wave propagation), Rayleigh instabilities can be supressed; resulting on uniform fibres [43]. Furthermore, visco-elasto-capillary theory sets boundaries for fibre spinnability that depend on several non-dimensional numbers describing the elastocapillary thinning rate in relation to the characteristic material's relaxation time. Usually, Deborah (De) and Onsager (Oh) numbers describe the electrospinnability of most polymers, when the condition $De \geq Oh \geq 1$ is met [11-14].

Oligosaccharides are carbohydrates that consist of monosaccharide units linked together to form short chains of varying length (di-, tri-, tetra-, pentasaccharides, *etc*.). Oligoaccharides have multiple chiral centres, including the anomeric centres of each monosaccharide unit. Each monosaccharide unit (6 carbons) may exist in either the pyranose (6-ring) or furanose (5-ring) form [15]. Saccharides which possess a terminal hemiacetal group are commonly denoted as reducing sugars, as these readily undergo mutarotation, a process which involves ring opening to the acyclic aldehyde and subsequent re-closure, equilibrating the diastereomeric α and β isomeric forms [15-17]. Similarly, the facile ring opening of reducing sugars allows equilibrium between pyranose and furanose forms, meaning that in aqueous solution a small amount of the open chain aldehyde is invariably present.

Polysaccharide concentrations leading to ten times the chain entanglement condition (*i.e.* 2 entanglements per chain) are able to form uniform fibres during electrospinning [20]. Also, it

is believed that the potential of saccharides to create metastable "supramolecular-like' architectures may underpin the electrospinnability of such materials [18, 19]. For example, the presence of hydrogen bonding is thought to influence the electrospinnability of food-grade polysaccharide solutions [20-22]. Likewise, non-covalent interactions between cyclodextrin (CD) molecules and hydrocolloids are thought to be responsible for the electrospinnability of highly concentrated aqueous solutions of CDs [23-30]. As evidence by Uyar *et al.,* who demonstrated that α-, β- and γ-CDs and their derivatives may be electrospun into continuous fibres in spite of their low molecular weight (972-1297 g/mol) [26]. Moreover, the authors proposed that the formation of molecular aggregates of aqueous CDs, can be attributable to extensive hydrogen bonding; a critical mechanism allowing the formation of α-, β- and γ-CDs fibres during electrospinning [24-26]. Bounded water on CDs aqueous solutions was reported be as high as 100% for solutions over 60% CDs wt. % concentrations, and as suggested by the authors, electrospinnability by depletion flocculation was the driving mechanism for the observed results [23].

The present authors recently reported that mono-, di- and tri-saccharide solutions exhibit reversible gel-like behaviour with a molecular cohesion that permits the electrospinning of these saccharides [31]. In the present work, the electrospinnability of aqueous solutions of reducing (glucose, fructose) and non-reducing (sucrose) saccharide solutions is investigated. Both single component solutions and mixtures of the saccharide solutions were examined to determine the effect of composition and concentration on the electrospinnability of saccharides. The saccharide concentration in aqueous solution was either under-saturated (-SAT), saturated (SAT), or super-saturated (+SAT). The electrospinnability of the saccharide solutions was then compared with the chain entanglement and visco-elasto-capillary theories that are typically used to model the electrospinnability of polymers. New experimental

evidence is provided on the electrospinnability of non-polymeric saccharides that might have implications for the development of new bio-nanomaterials for medical, food and pharmaceutical applications [21, 30].

2. Experimental procedures

2.1 Materials and solution preparation

D-glucose ($C_6H_{12}O_6$, > 99.5 %, CAS # 50-99-7), D-sucrose ($C_{12}H_{22}O_{11}$, > 99.5 %, CAS # 57-50-1) and D-fructose ($C_6H_{12}O_6$, > 99%, CAS # 57-48-7) were used as supplied (Sigma-Aldrich, Germany) without further purification. Various under-saturated, saturated and super-saturated solutions composed of single, binary and ternary combinations of glucose, fructose and sucrose were prepared for electrospinning. The super-saturated solutions were prepared by increasing the dissolution temperature to 75 ± 2 °C for short periods of time, and then promptly storing the solutions at lower temperatures (50 ± 2 °C) on air-tight sealed container to avoid precipitation. Solutions were prepared, processed and characterized in triplicate. Density was measured on a Mettler-Toledo (XPE) analytical microbalance. The naming of the various solution compositions was abbreviated as follows: glucose (G), fructose (F), sucrose (S), glucose-fructose-sucrose (GFS), glucose-fructose (GF) and glucose-sucrose (GS). Additionally, the samples were labelled according to the concentration regime: under-saturated (-SAT), saturated (SAT) and supersaturated (+SAT). For example, FS/+SAT indicates a supersaturated solution with equal amounts of both fructose and sucrose.

2.2 Physical properties of the electrospinning solutions

The average electrical conductivity and surface tension of the solutions were measured in triplicate at a temperature of 50 ± 2 °C. The surface tension was measured using an optical goniometer (KSV CAM200, KSV Instruments Ltd., Finland). The electrical conductivity of

the solutions was measured using a conductivity meter (EDT Instruments, RE387TX, Dover, United Kingdom), with a claimed precision of ± 0.5 %.

2.3 Rheological characterization of electrospinning solutions

The rheological behaviour of saccharide solutions was measured using an Anton-Paar Physica MCR 310 Rheometer (Anton Paar, Australia). All experiments were performed with a cone and plate geometry (CP50–2) with a diameter of 50 mm and an angle of 2° at a constant temperature of 50 ± 1 °C. The Dynamic viscosity (μ) of the saccharide solutions was measured in both oscillatory and flow tests with shear rates ($\dot{\gamma}$) or varying frequencies from 0.1 to 1000 s^{-1}. A strain of 0.1 % was determined to be within the linear viscoelastic range of the solutions as determined from a strain sweep measured at a frequency of 1.5 Hz. The zero-shear viscosity was determined from the complex viscosity data obtained by oscillatory tests using the standard Cox-Merz relation at an average shear rate of 0.1 s^{-1}. The storage (G') and loss (G'') moduli were measured in oscillatory mode over an angular frequency (ω) range of 0.1-1000 s^{-1}. However, shear viscosity and storage moduli (G') data, is only reported for saccharide /+SAT solutions, as lower concentrations did not show a marked difference on the measured rheological properties.

2.4 Electrospinning procedure and characterization

A syringe pump (NE-500, New Era Pump Systems Inc., NY, USA) was used to deliver the electrospinning solution to the spinneret (metal hypodermic syringe needle, internal diameter of 0.3 mm) at a flow rate of 0.3 µl/min. All of the solutions were too viscous to be delivered to the spinneret at room temperature (20 °C). Thus, all solutions were supplied to the spinneret at a temperature of 50 ± 2 °C to facilitate the delivery of the solution to the spinneret. The electrospinning apparatus was enclosed in a grounded Faraday cage at a

temperature and relative humidity of 35 ± 1 °C and 38 ± 3 %, respectively. Electrospinning of the various solutions was performed using an applied voltage of +15 kV and a spinneret-to-collector distance of 15 cm, resulting in an electric field strength (*E*) of 1 ± 0.02 kV/cm. All solutions were supplied to the spinneret at a temperature of 50 ± 2 °C; via a heated glass syringe with a temperature controlled coil, since the solutions were too viscous to be delivered to the spinneret at room temperature (20 °C). The polarity of the applied voltage was not found to influence the electrospinnability of any of the saccharide solutions. A high-speed motion camera (MotionPro® X3) with sensitivity of 1280 × 1024 pixels was used for capturing photographic images of the jet during flight. The fibre in flight was illuminated during video capture by 6 × 12 V/50 W halogen lamps. Electrospun specimens were collected using a grounded aluminium foil substrate and subsequently stored in a temperature-controlled vacuum desiccator with a relative humidity content of 10% ± 2% prior to characterization by microscopy. The microstructures of the electrospun samples were examined with scanning electron microscopy (SEM, JEOL JCM-5000 NeoScope Tokyo, Japan). Specimens were observed by secondary electron imaging without the use of a conductive coating at an accelerating voltage of 10 kV in high vacuum mode.

3. Results and discussion

3.1 Electrospinnability of concentrated saccharide solutions.

Fructose and Sucrose /SAT and /+SAT solutions and their combinations, showed the best electrospinnability results, in comparison with Glucose containing solutions (Figures 1 and 2). However, both Glucose and Fructose /SAT and /+SAT solutions showed filament formation (Figure 2). Likewise, the ternary combination of Glucose, Sucrose and Fructose /+SAT solution also showed filament formation (Figure 3). In contrast, both Glucose and Sucrose /SAT and /+SAT solutions did not show any filament formation (Figures 1 and 2).

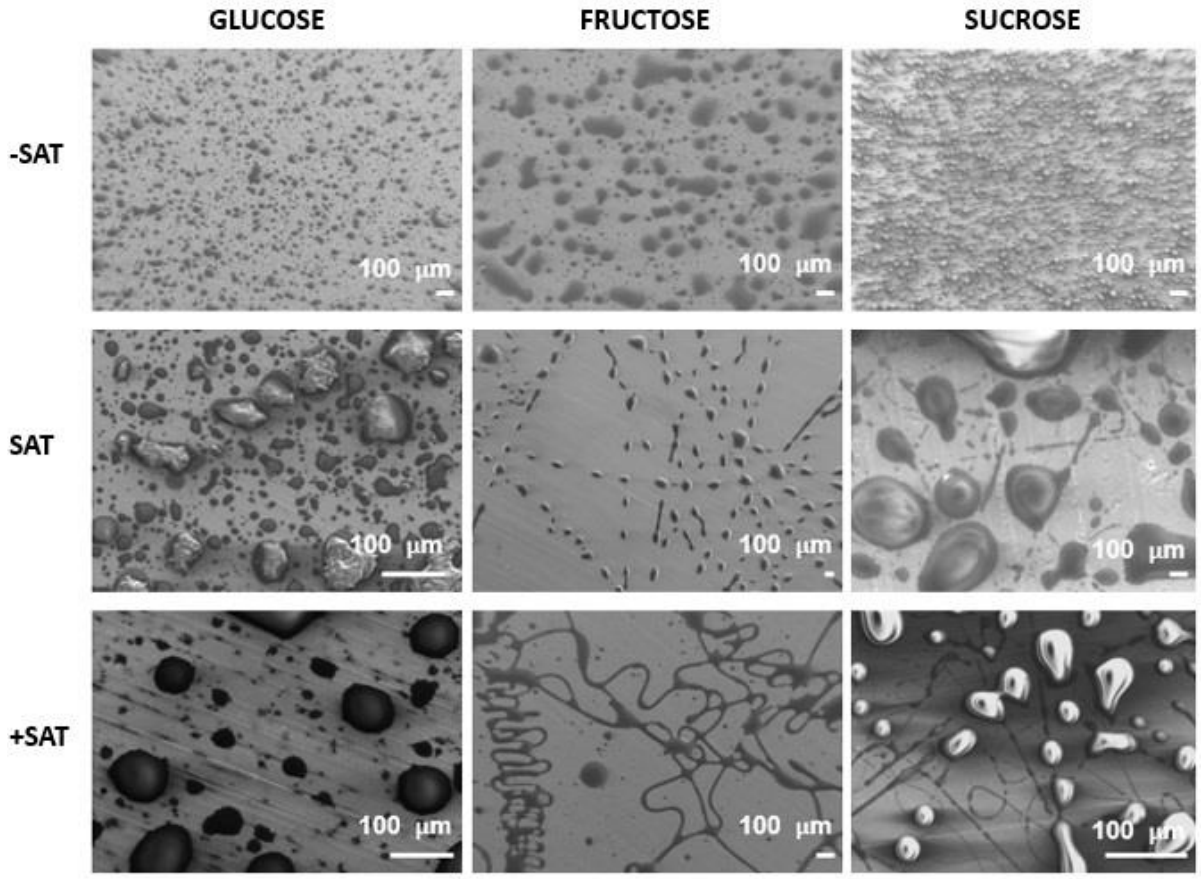

Figure 1. Electrospun sub-micron filaments of single saccharide solutions at 50 ˚C.

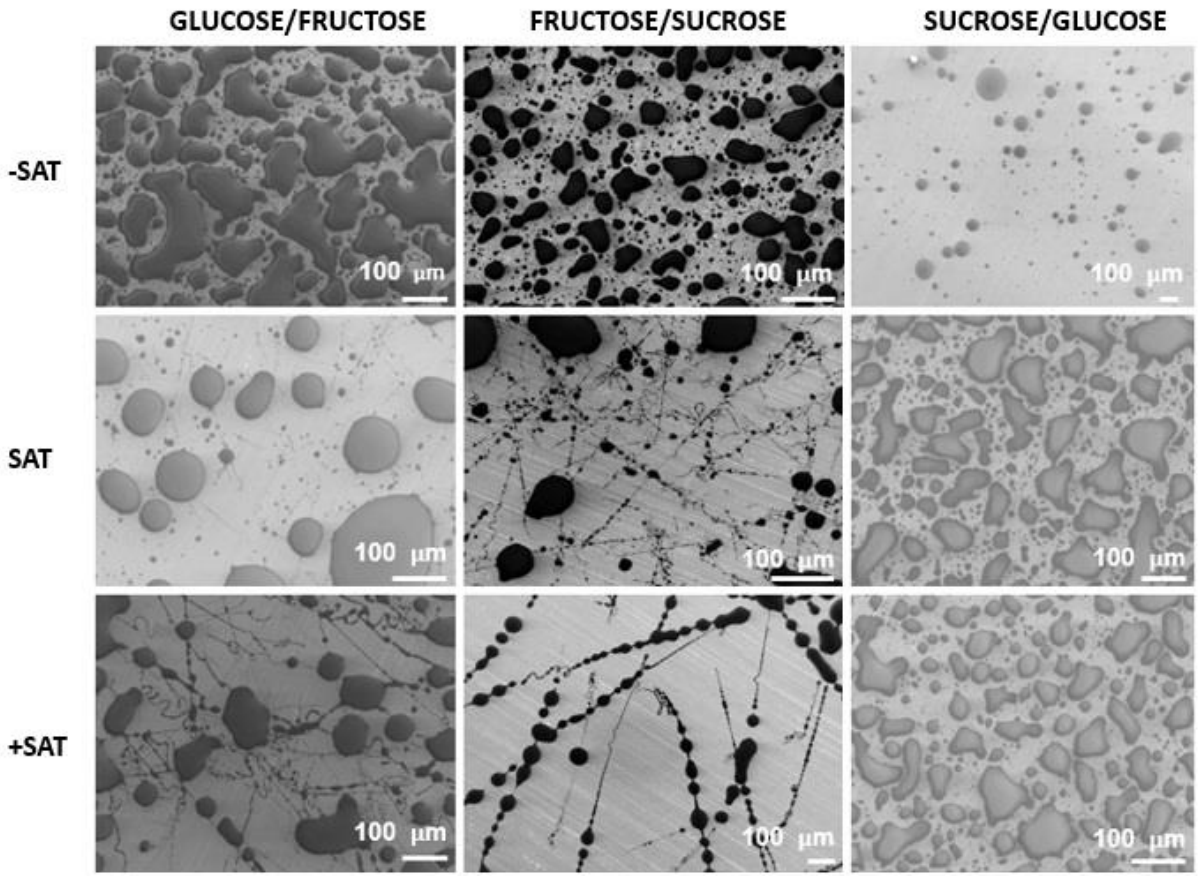

Figure 2. Electrospun sub-micron filaments with binary combinations of saccharide at 50 ˚C.

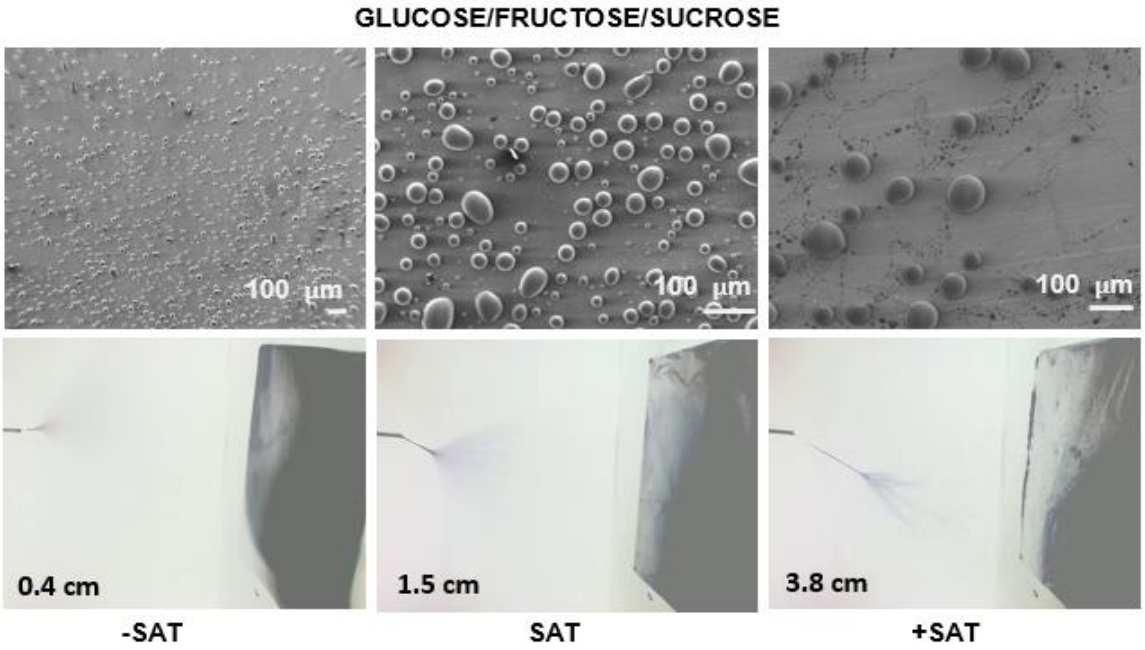

Figure 3. Electrospun sub-micron filaments and electrospinning of solutions with ternary combinations of saccharide at 50 ˚C.

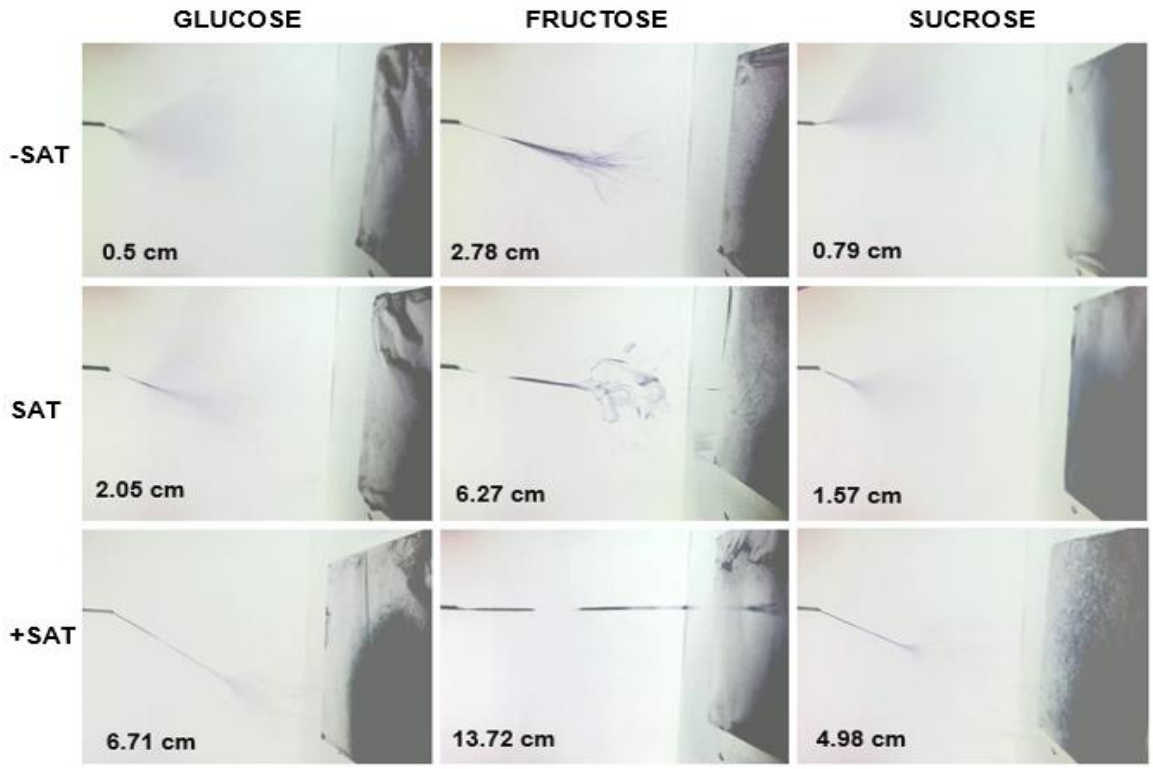

Figure 4. Electrospinning of single saccharide solutions at 50 ˚C.

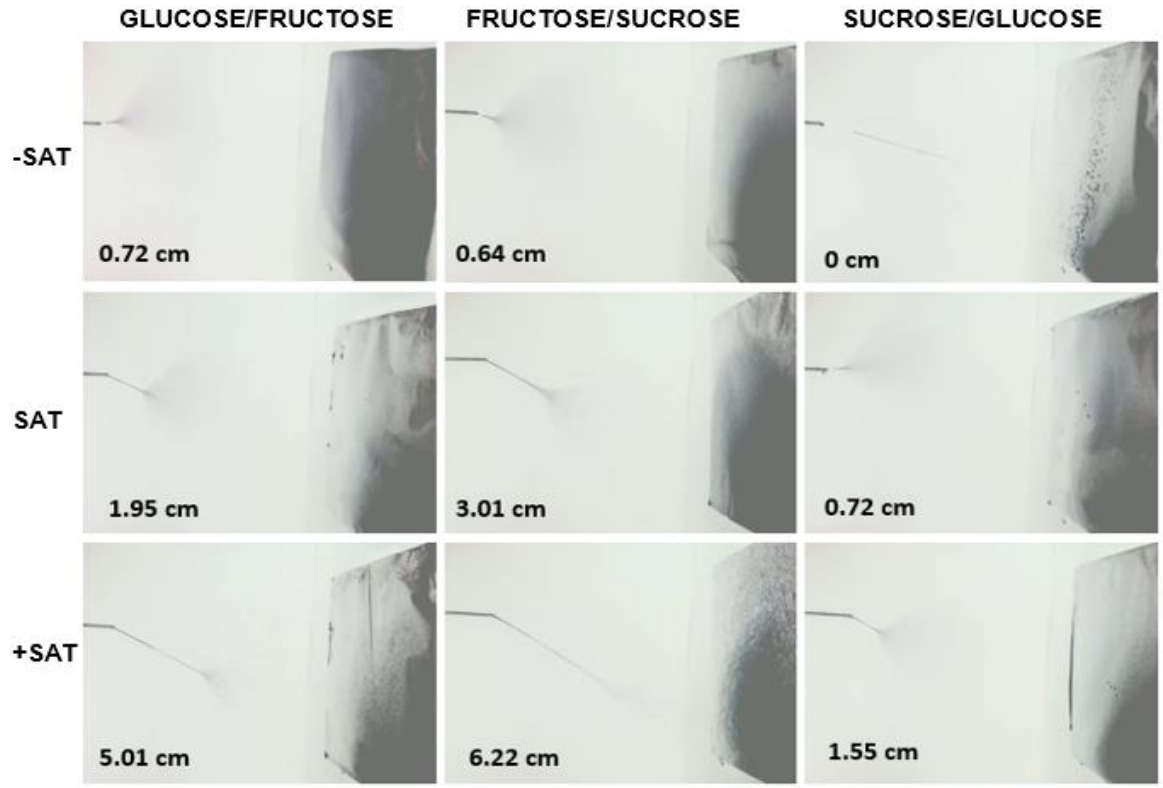

Figure 5. Electrospinning of solutions with binary combinations of saccharide at 50 ˚C.

Both stable jet formation and chaotic whipping instability was observed for most sucrose containing solutions at super saturated concentrations (Figures 3-5). However, no stable jet formation was observed for SG/-SAT (Figure 5). In particular F/+SAT showed the longest straight jet and the best electrospinnability behaviour for single saccharide solutions, as evidenced by their continuous filament formation (Figure 1 and 4). Although highly hydrophilic, FS/+SAT filaments remained stable in geometry after several days.

3.2 Effect of saccharide concentration and composition on the physical properties of aqueous solutions

The highest density (1.61 g/ml), electrical conductivity (4.39×10^{-4} S/m), and surface tension (12.109 N/m) was found for FS/+SAT, GFS/-SAT, and GS/+SAT, respectively. In contrast, the lowest density (1.36 g/ml), conductivity (0.03×10^{-4} S/m), and surface tension (7.687 N/m) was found for G/-SAT, F/+SAT, and G/-SAT, respectively. Higher densities related to greater electrospinnability (Figure 6). In contrast, lower conductivities at higher concentrations promoted filament formation (Figure 8). However, no obvious relationship between surface tension and electrospinnability was observed (Figure 7). The average standard deviations for the density, conductivity and surface tension were 0.0617 g/ml, for 0. 228 10^{-4} S/m and 0.4457 N/m, respectively. Circled areas on all graphs (Figures 6-10) exhibited the highest electrospinnability, taken as the formation of the longest continuous non-beaded filaments with stable jet formation.

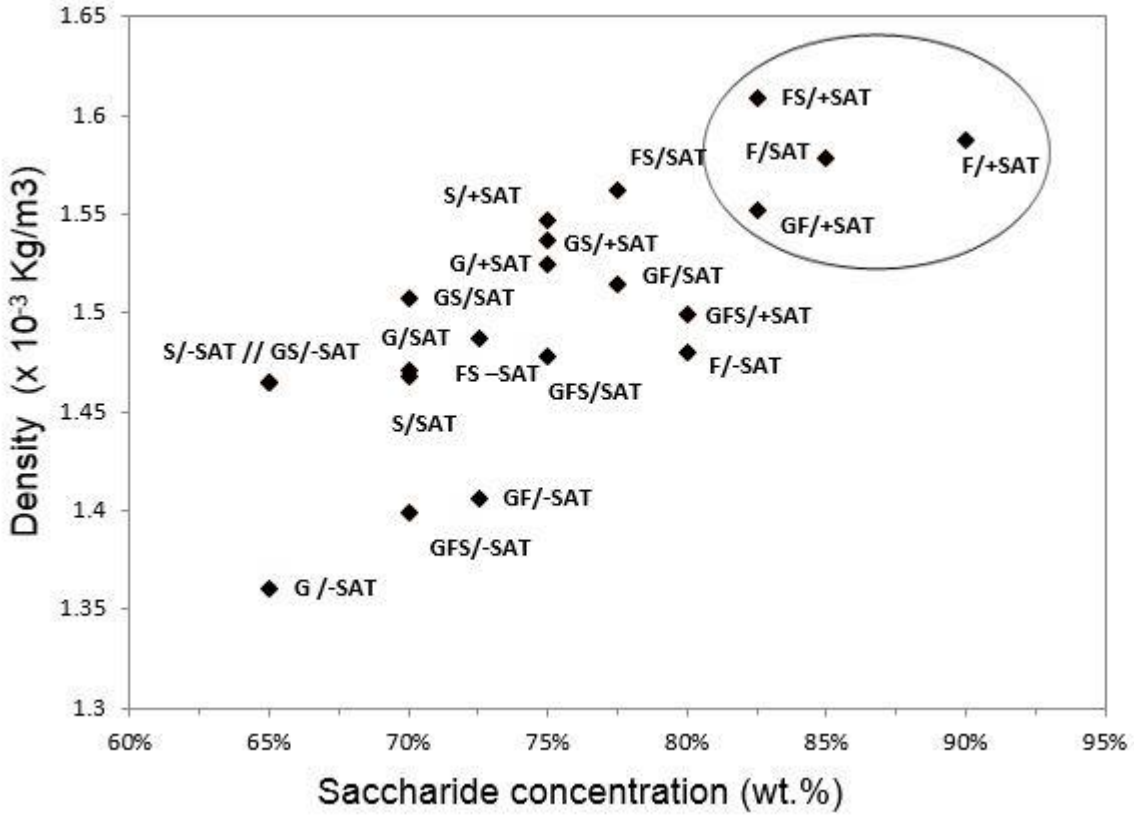

Figure 6. The density of the aqueous saccharide solutions as a function of the saccharide concentration at 50 ˚C. Circle indicates those solutions with improved electrospinnability (greater filament formation). The average standard deviation for the density was 0.0617.

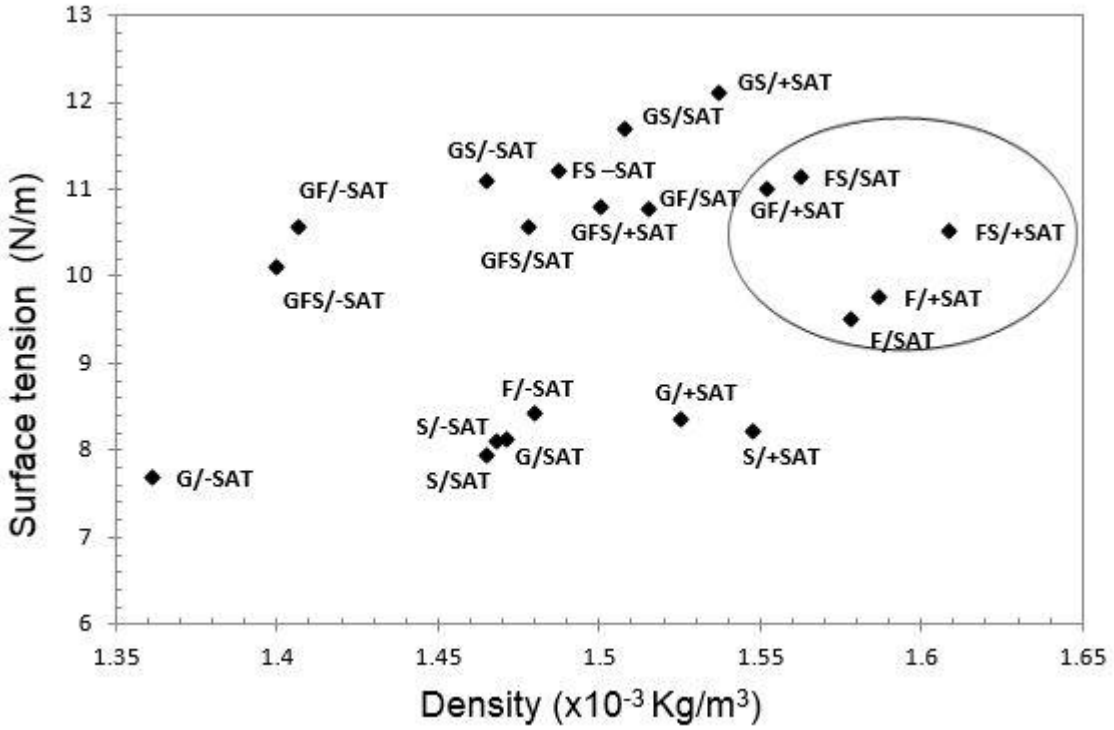

Figure 7. Surface tension as a function of density at 50 ˚C. Circle indicates those solutions with improved electrospinnability (greater filament formation). The average standard deviation for surface tension was 0.4457 N/m.

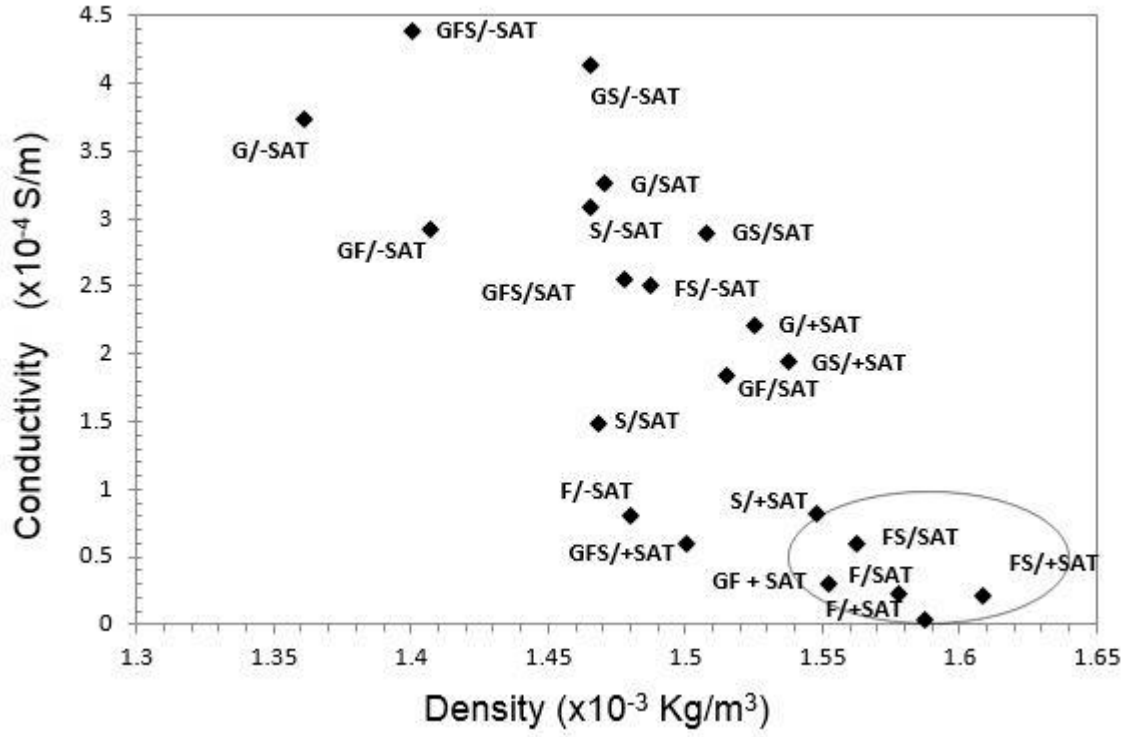

Figure 8. Conductivity as a function of density at 50 ˚C. Circle indicates those solutions with improved electrospinnability (*i.e.* higher filament formation). The average standard deviation for conductivity was 0. 228 10^{-4} S/m.

In contrast to the expectation that relatively higher conductivities correspond to higher ionic mobility, hence increased electrospinnability, samples with lower conductivities electrospun best (Figure 8) [7-9]. Lower conductivity values could suggest that charge during electrospinning, might not be entirely transported by ionic diffusion. Likewise, longer jet lengths (Figures 3-5) were observed to correlate with formation of continuous filaments, or enhanced electrospinnability (Figure 1-3).

3.3 Effect of solution viscosity on the stable jet length

Surface tension and conductivity are important factors for the electrospinnability of any given material, in addition to visco-elasticity. This is especially the case for many bio–polymers and supramolecular polymers which rely on secondary forces to electrospin, rather than covalent entangled chains [32-35]. For example, hydrogen bonding can have a significant effect on capillary driven processes [36-40]. Also, longer relaxation times of some supramolecular polymer solutions, can be associated with higher electro-visco-elasticities, often resulting on improved electrospinnability [41, 52]. Often, such behaviour could be explained by the sticky reptation model of associating networks, which proposes that fast reversible (short-term) bonds in supramolecular polymers, such as hydrogen bonds, can act as "sticky points" for the so called "associative supramolecular networks", and so dictate the long-term stress and strain dynamics of the bulk solution [49]. In other words, concentrated saccharide solutions could behave as an interconnected network or gel, for time scales shorter than the lifetime of these reversible bonds (*i.e*. hydrogen bonding) [49]. Moreover, it is

known that increased jet length or electrospun threads may indicate a polymer solution with a higher elasticity [42-47]. The associated electrospinnability for visco-elastic polymer systems is also found on non-polymeric systems, as supported by the relationship between higher zero-shear viscosities, longer stable jet lengths (elasticity) and electrospinnability of tested saccharide solutions (Figures 9 and 10).

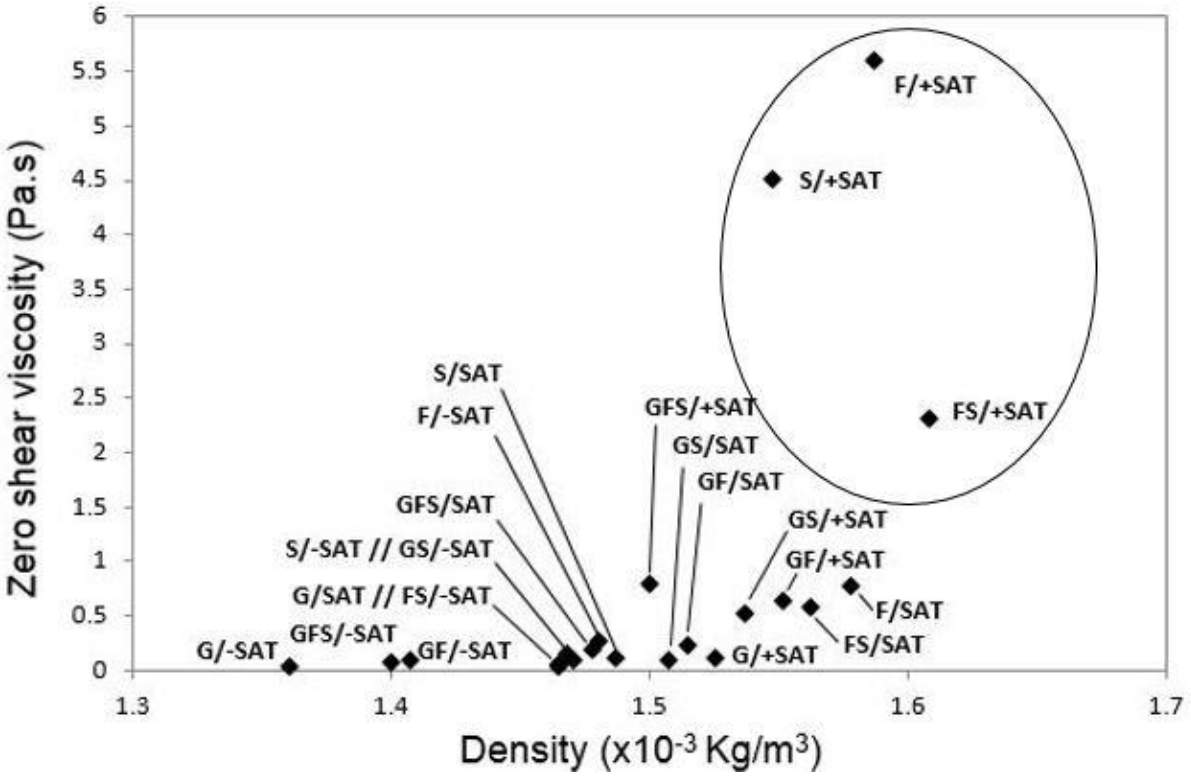

Figure 9. Zero shear viscosity as a function of density at 50 ˚C. Circle indicates those solutions with improved electrospinnability (greater filament formation).

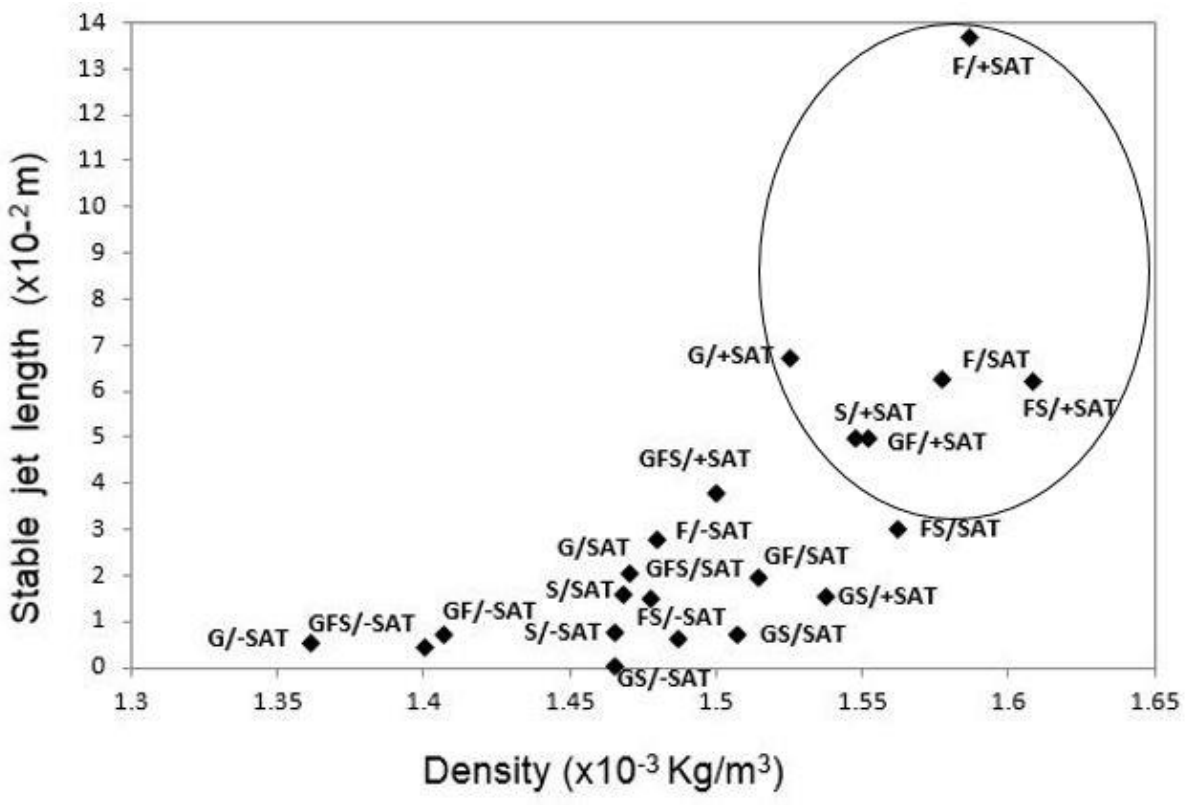

Figure 10. Stable jet length as a function of density at 50 ˚C. Circle indicates those solutions with improved electrospinnability (greater filament formation).

Furthermore, elasticity for supramolecular polymers is often related to electrospinnability, through gelation or colloid aggregation *via* a hydrogen bonding network [41, 48, 49]. Also, viscoelasticity plays an important role in the electrospinnability of cyclodextrins [23, 26]. For example, Uyar *et al.* proposed that hydrogen bonding promotes the self-assembly of CD molecules into aggregates, resulting in solutions of high elasticity and thus, enhanced electrospinnability [26]. Similarly, sucrose in aqueous solutions can strongly bind water molecules in its hydration sphere, orienting water molecules even at long distances, as in hydrocolloids clusters, a characteristic behavior of supramolecular polymers [15-17, 50].

3.4 Viscoelasticity of saccharide solutions

Viscosity values measured for saccharide solutions were relatively lower when compared with typical polymeric materials usually measured at 20 ˚C, since the associated dynamic shear viscosities for tested saccharide solutions did not exceeded 10 Pa.s at 50 ˚C (Figure 11). Moreover, Figure 11 show that most solutions containing fructose and sucrose behaved like non-Newtonian fluids. These results are in agreement with previous reported evidence from Quintas *et al.*, who reported that nucleation and crystal growth during rheology of metastable supersaturated sucrose aqueous solutions does not correlate with the expected Newtonian behaviour theoretically predicted by Arrhenius models [51]. However, further understanding the effects of such nucleation processes is needed, in order to better understand the associated colloid aggregation and self-assembly processes that drives the electrospinnability of concentrated saccharide solutions [19, 26, 31].

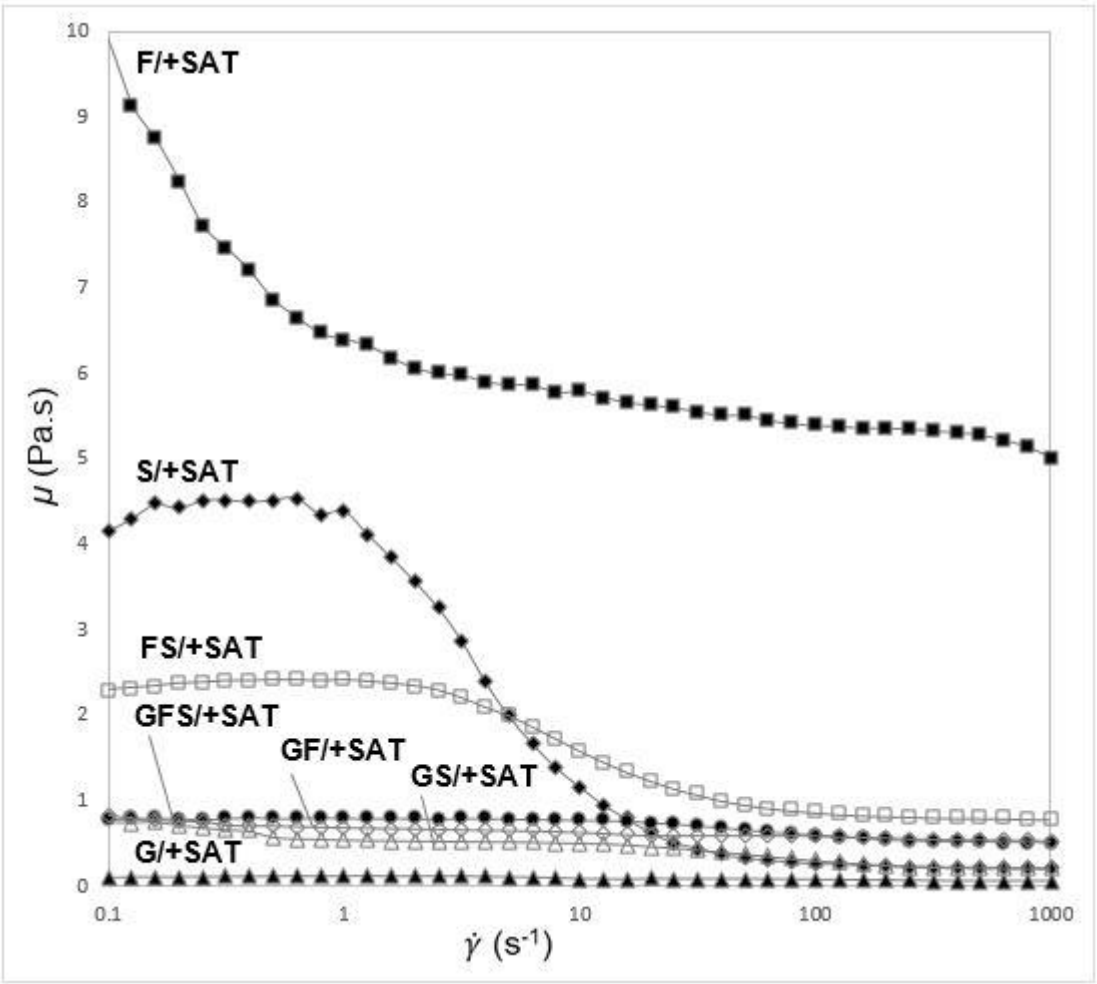

Figure 11. Shear rate ($\dot{\gamma}$) to dynamic viscosity (μ) relationship for single and ternary combination of saccharide at 50 ˚C.

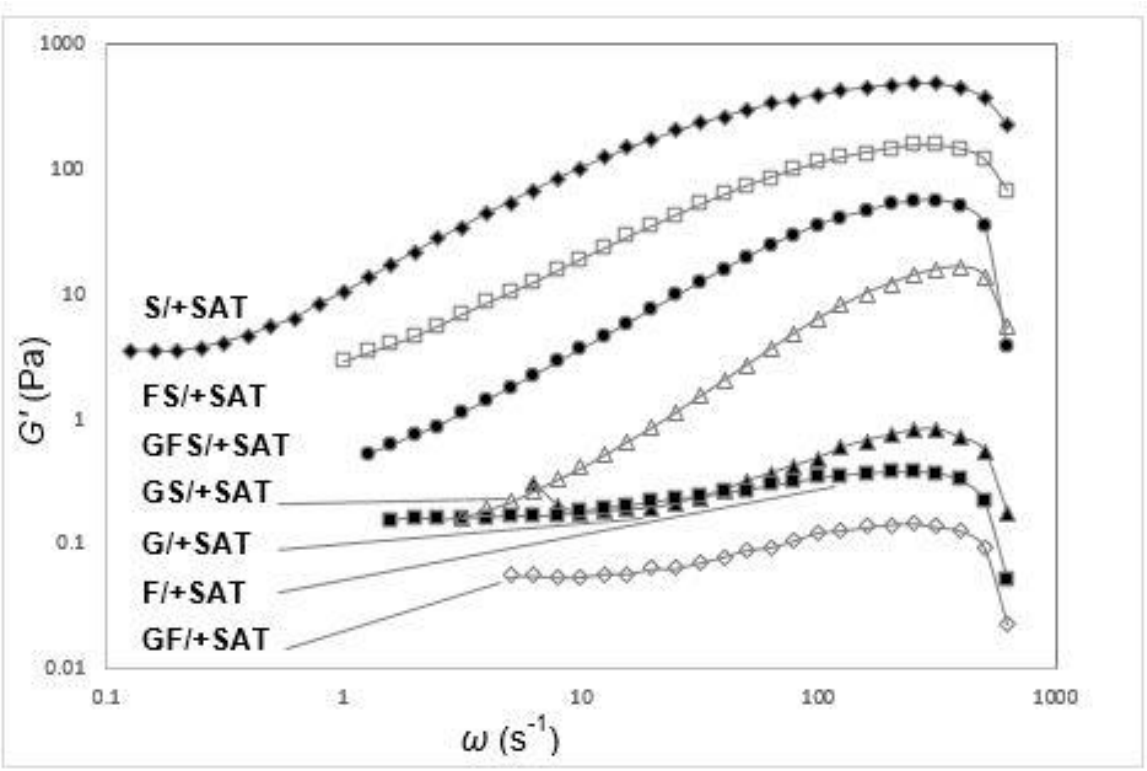

Figure 12. Angular Frequency to storage modulus (G') relationship for single and ternary combination of saccharide at 50 ˚C.

The non-Newtonian behaviour of the non-reducing sugars is especially noticeable for the sucrose and fructose-sucrose super saturated solutions as evidence by the shear thinning behaviour of FS/+SAT (Figure 11). Also, all samples were more viscous than elastic due to the G' values being always lower than their respective G'' (not shown). However, S/+SAT showed the highest G' at higher angular frequencies while F/+SAT showed the lowest G' at all angular frequencies (Figure 12). Likewise, binary mixtures of sucrose solutions showed higher G' at all angular frequencies, while GF/+SAT showed the lowest G' of all solutions (Figure 12). Moreover, F/+SAT which exhibited the longest stable jet length (Figure 4), also showed the second lower G' of all solutions. This apparent contradictory behaviour may be

associated with the non-linear additivity of hydrogen bonding forces when subjected to external electric fields [52, 53]. For example, when aqueous solutions of non-polar molecules are subjected to high voltage electric fields, electron-dynamic interactions-Liftshitz-van der Waals; arising from permanent dipole-dipole interactions (Keesom), dipole-induced dipole (dispersion) interactions -London forces, and dipole-induced dipole (induction) interactions-Debye forces, can promote an asymmetric electronic configuration of the molecules within the solution [52, 53].The orientation of charged water molecules can be in turn associated to the high density of opposing electron-donors, often a sizeable distance away from the hydrophobic (electron donating) surfaces, related to the net Liftshitz-van der Waals interactions between molecules [52, 53]. These results are in agreement with literature on the electrospinnability of food grade polysaccharide [20], also correlating to higher Trouton ratios (the ratio of extensional viscosity to shear viscosity). This further suggests that rheological elasticity (storage modulus > loss modulus) could be an important property for the electrospinnability of most saccharide solutions.

However, neither critical concentration nor elasto-visco capillary theories consider such molecular properties on their respective electrospinnability models. Hence, experimental data was compared with chain entanglement and visco-elasto capillary theories, to further understand the validity of such models when applied to non-polymeric electrospinnability systems [6, 11].

3.5 Electrospinnability models

3.5.1 Critical concentration - chain entanglement

The stable formation of polymer fibres during electrospinning requires > 2 entanglements per chain to provide sufficient molecular cohesion, according to the chain entanglement theory.

The critical overlap concentration (c^*) may be calculated using Equation 1, where M is the molecular mass, N_a is Avogadro's number, and $\langle r^2 \rangle^{3/2}$ is the root-mean-square end-to-end distance.

$$c^* \approx \frac{3M}{4\pi * [(r^2)^{3/2}] * N_a} \qquad \text{Equation 1}$$

Macromolecules with low molecular mass and many peripheral hydroxyl groups (*i.e.* high hydrophilicity) cannot be described by an end-to-end distance due to fluctuations in their hydration shells [40]. Consequently, the use of the hydrodynamic radius (R_h) offers a more accurate representation of molecular dimensions than the root-mean-square end-to-end distance as given by Equation 2.

$$R_h = \sum_i^n 2\left(\frac{r/n}{\sqrt{2\pi}}\right) \qquad \text{Equation 2}$$

Using open source software Avogadro 2.0 as the computational method to model the van der Waals molecular ratio for each saccharide molecule, the Merck Molecular Force Field (MMFF) for sucrose, glucose and fructose, through a standard geometry optimization was calculated. Subsequently, an approximate hydrodynamic radius (R_h) of the glucose, fructose and sucrose molecules was determined by averaging the linear distances between each carbon and peripheral hydrogen and oxygen atom (Figure 13) [40, 45-47]. The critical overlap concentration $(c^*)^*$ was then calculated using Equation 1 (Table 1).

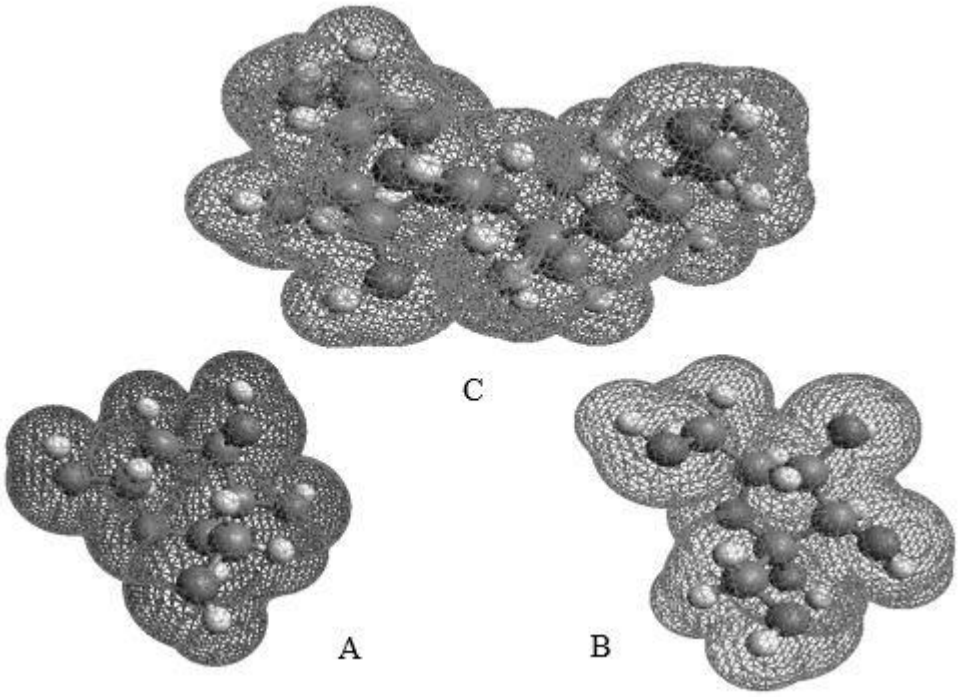

Figure 13. Molecular models showing their van der Waals molecular ratios for glucose (A), fructose (B) and sucrose (C).

Based on the presented evidence, the critical concentration model applied to electrospinning confirms the electrospinnability of tested saccharide solutions with a critical entangled (C*e*) concentration (*Ce* ~10 × *c**) of only 2 × *c**. In contrast, critical concentration theory for polymers predicts a critical entangled concentration orders of magnitude higher than the critical overlap concentration (*c**) found for tested saccharide solutions (Table 1). These results suggest that the electrospinnability of non-polymeric systems can be achieved with less than 2 × *c**. Thus, the chain entanglement condition of 2 × *Ce* (where *Ce* = 10 × *c**) does not predetermine electrospinning of the non-polymeric systems examined in the present work, as is in the case of polymeric solutions. Presumably, the electrospinning of non-polymeric systems relies on other non-physical intermolecular interactions that influence their complex viscoelastic properties, such as Van der Waals forces and hydrogen bonding mechanisms.

Table 1: Critical overlap concentration values for all solutions based on the hydrodynamic radius (R_h)

Parameter	Solution						
	G	F	S	GFS	GF	GS	FS
M (g/mol)	180. 2	180. 2	342. 3	210. 6	180. 2	236. 9	228. 8
R_h (Å)	2. 5	3. 1	6. 2	3. 9	2. 8	4. 4	4. 7
c^* (wt. %)	291. 1	151. 2	36. 8	90. 2	203. 7	72. 9	56. 1

3.5.2 Visco-elasto-capillary theory

Numerous models from polymer physics, rheology and fluid dynamics have been developed to explain the behaviour of non–Newtonian polymer jets [42-44]. Some of these models have been applied to electrospinning and incorporate the electro-capillary effects as well as the viscoelastic properties of the material. Electrospinnability predicted by these models depend on the growth of a visco-elasto-capillary wave, similar to the Rayleigh instability that scales with λ^{-1}, where λ is the characteristic polymer relaxation time [14, 43]. Thus, the Deborah number must be greater than 1 for stable fibre formation [14]. The relationship between visco-elasto-capillary theory and jet formation is summarised in Figure 14.

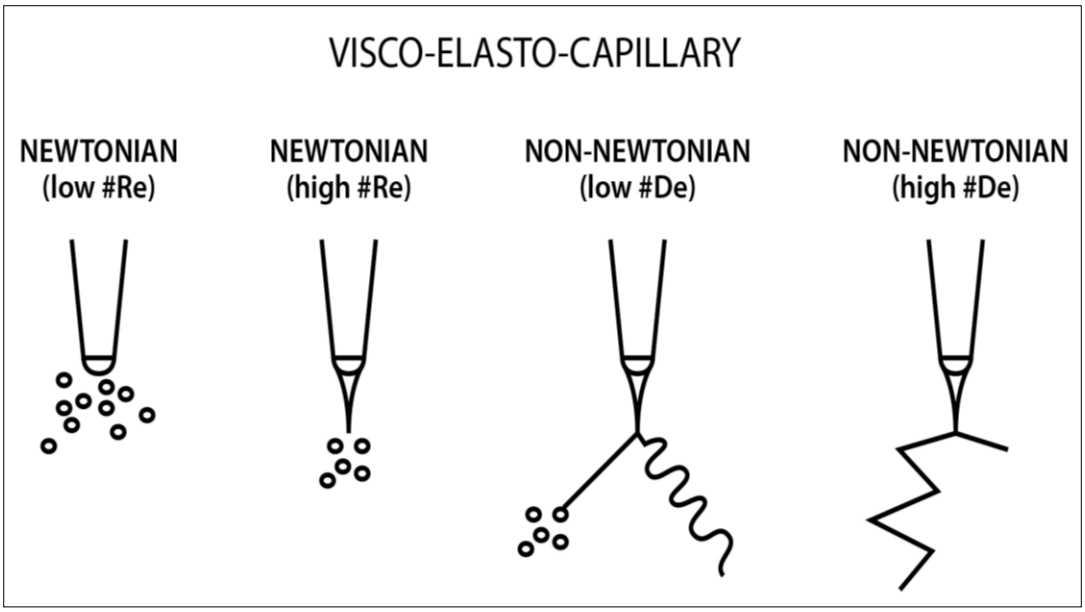

Figure 14. Representation of the visco-elasto-capillary theory and its correlation to jet formation, showing the transition from intermittent spraying (low # Re), stable electrospraying (high #Re), electrospraying and electrospinning (low #De) and stable spinning (high #De). Re is the Reynolds number ($Re = (\rho LV\_avg)/\mu$) and De is the intrinsic Deborah number (De = stress relaxation time / time of observation).

On a capillary thinning process such as electrospinning, surface tension drives the thinning and either viscosity or elasticity resist necking. Therefore higher #De and #Re are needed for electrospinnability, since both imply that a higher or longer relaxation time of the overall system is present in respect to the capillary perturbation wavelength [14, 42-44]. Moreover, the longest Rouse relaxation time for polymers is usually in the range of 1 to 3 s. Relaxation process that occur on smaller time scales than 10-100 ms cannot be unambiguously resolved [14]. Hence, Rouse relaxation times are often inaccurate when predicting stress relaxation in processes with large strains in very short times (typical of electrospinning), since the effective time for the molecules to relax the applied stresses is typically less than 1 ms [14]. Consequently, a simplified version of the tube model *i.e.* ($\lambda = k(G')/k'(G'')$ was used in this study for approaching the longest relaxation times of the solutions; where k is a constant

derived from the respective best linear and square fitting of the storage ($G'=k\omega$) and loss modulus ($G''= k\omega^2$) to the angular frequency (ω). Approximate values were then used to estimate the dimensionless numbers (*i.e.* Reynolds, Capillary, Weber, Elasticity, Ohnesorge, and Weissenberg) required to find the intrinsic Deborah number as described by the visco-elasto-capillary theory, and as proposed by McKinley *et al*. (Figure 15) [11, 13, 14].

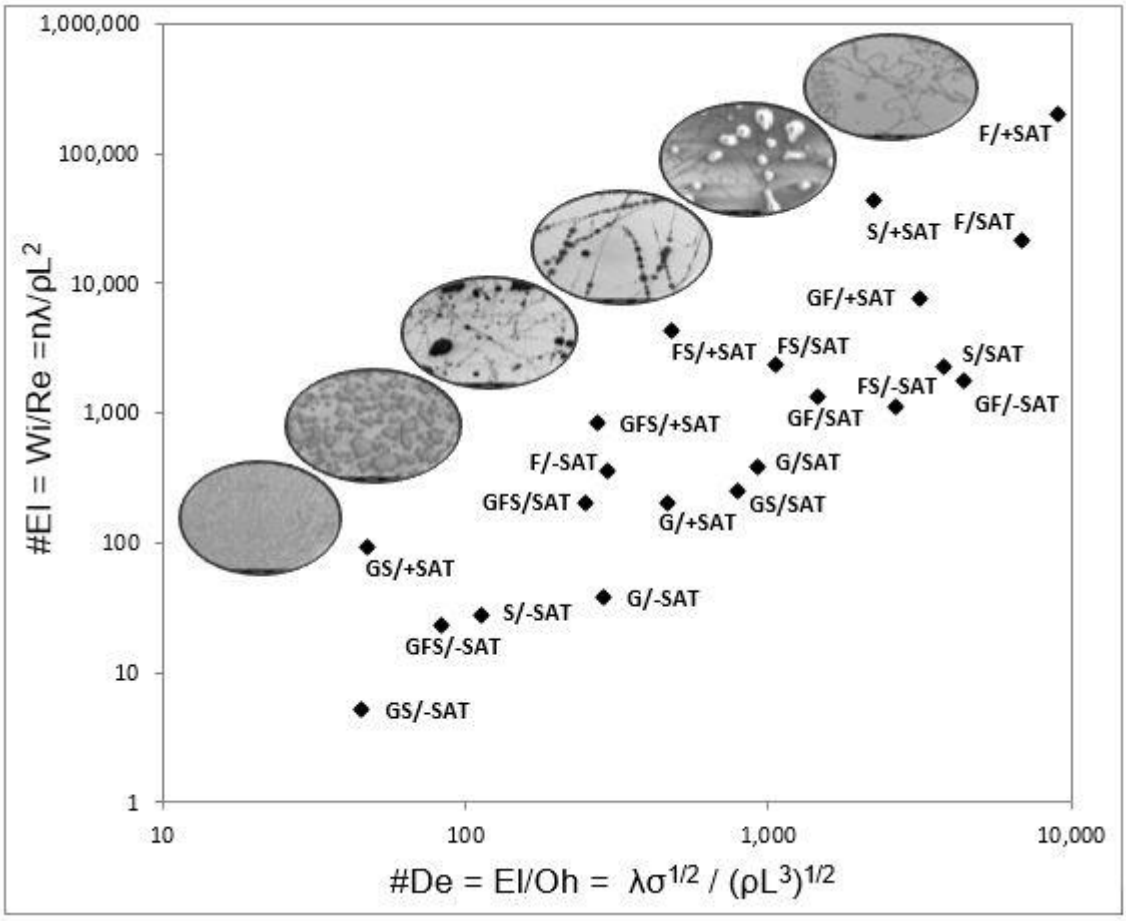

Figure 15. Logarithmic scale of the elasto-capillary numbers plotted against the intrinsic Deborah numbers for all saccharide solutions, at all concentrations at 50 ˚C.

Based on the intrinsic Deborah and elasto-capillary number relationship, the visco-elasto-capillary theory provides a better description than the chain entanglement model of the behaviour exhibited by saccharide solutions used in the present work (Figure 15). Further

supporting a correlation between increased electrospinnability and higher Deborah and elasto-capillary numbers for tested saccharide solutions. However, visco-elasto capillary theory does not offer an explanation as to how bounded water and aqueous phase separation (aggregate formation) relates to hydrogen bonding interactions and jet charge transport mechanisms [55-58]. Non-the less, visco-elasto capillary theory suggests that longer relaxation times or the capacity to remain electrically stressed for longer periods of time, correlated to a higher electro-visco-elasticity, resulting on improved electrospinnability.

4. Conclusions

New experimental findings on the electrospinning of sugars are reported. Relationships between the physical-chemical properties of the solutions and their associated visco-elastic behaviour are discussed. The following electrospinnability trends were observed throughout the experimentation.

- Higher density solutions promoted electrospinnability, super saturated > saturated > under saturated concentrations (Figure 6).
- Higher than averaged surface tension values at higher concentrations also promoted electrospinnability (Figure 7).
- Lower conductivities at higher concentrations also promoted electrospinnability of sugars (Figure 8).
- Zero shear viscosities (Figure 4) and longer stable jet lengths (Figure 10) can be also regarded as indicators for the electrospinnability of tested materials.
- Electrospinnability was also promoted by high shear viscosities at lower shear rates and higher G' at high shear rates ($G' > G''$) (Figures 11 and 12).

In general, visco-elasto capillary theory offers a reliable prediction of the electrospinnability of saccharide solutions. However, it is still not clear how electrospinnability relates to the hydrogen donor and hydrogen acceptor interactions, Debye's length and other complex electrodynamic interactions caused by the high voltages that drive the electrospinning process.

Acknowledgements

The authors thank the Ministry of Business Innovation and Employment of New Zealand (MBIE) for financial support. Author (PGTL) is particularly grateful to the National Institute of Science and Technology of Mexico (CONACYT) for financial assistance. The technical assistance from the NZ Institute for Plant and Food Research Ltd., Mr Neil Buunk of Electrospinz Ltd., and from Revolution Fibres Ltd. is also gratefully acknowledged.

Compliance with Ethical Standards

This study was funded by the University of Canterbury and Plant and Food Research Ltd., through a joint PhD studentship received from the Ministry of Business Innovation and Employment of New Zealand (MBIE) granted through Revolution Fibres Ltd., and by a PhD scholarship from the National Institute of Science and Technology of Mexico (CONACYT) granted to Pablo Lepe. No private funding was received from any other Company or external organization. All authors declare that there is no conflict of interest related to the publication of this manuscript.

References

1. Reneker D, Yarin A: Electrospinning jets and polymer nanofibers, Polymer, 49 (2008) 2387-2425.
2. Doshi J, Reneker D: Electrospinning Process and Applications of Electrospun Fibers, Journal of Electrostatics, 35 (1995) 151-160.
3. Greiner A, Wendorff J: Electrospinning: A Fascinating Method for the Preparation of Ultrathin Fibers, Angewandte Chemie International Edition, 46 (2007) 5670-5703.
4. Tucker N, Stanger J, Staiger M, Razzaq H, Hofman K: The History of the Science and Technology of Electrospinning from 1600 to 1995, Journal of Engineered Fibers and Fabrics, Special Issue (2012) 63-73.
5. Spivak A, Dzenis Y, Reneker D: A Model of Steady State Jet in the Electrospinning Process, Mechanics Research Communications, 27 (2000) 37-42.
6. Shenoy S, Bat W: Role of chain entanglements on fiber formation during electrospinning of polymer solutions; good solvent, non–specific polymer–polymer interaction limit, Polymer, 46 (2005) 3372-3384.
7. Feng J: Stretching of a straight electrically charged viscoelastic jet, Journal of Non–Newtonian Fluid Mech., 116 (2003) 55-70.
8. Hohman M, Rutledge G, Brenner M: Electrospinning and electrically forced jets II, Applied Physics of fluids, 13 (2001) 2221-2236.
9. Reneker D, Yarin A, Fong H, Koombhongse S: Bending instability of electrically charged liquid jets of polymer solutions in electrospinning, Journal of Applied Physics, 87 (2000) 4531-4547.

10. McKee M, Garth L, Timothy EL: Correlations of Solution Rheology with Electrospun Fiber Formation of Linear and Branched Polyesters, Macromolecules, 37 (2004) 1760-1767.
11. McKinley G: Dimensionless groups for understanding free surface flows of complex fluids, Rheology Bulletin, (2005) 1-6.
12. Yu J, Rutledge G: The role of elasticity in the formation of electrospun fibers, Polymer, 47 (2006) 4789-4797.
13. McKinley G: Visco–Elasto–Capillary thinning and break–up of complex fluids. Hatsopoulos, Microfluids Laboratory–MIT report, (2005) 1-50.
14. Crest J, McKinley G: Formation of microfibers and nanofibres by capillary–driven thinning of drying viscoelastic filaments, MIT report, (2009) 1-43.
15. Pérez A, Macedo E: Prediction of thermodynamic properties of sugars in aqueous solutions: correlation and prediction using a modified UNIQUAC model, Fluid phase equilibria, 123 (1996) 71-95.
16. Fabri D, Williams M, Halstead T: Water t2 relaxation in sugar solutions, Carbohydrate research, 340, (2005) 889-905.
17. Jansson H, Bergman R, Swenson J. Dynamics of sugar solutions as studied by dielectric spectroscopy, Journal of non–crystalline solids, 351 (2005) 2858-2863.
18. Desiraju G, Steiner T: The weak hydrogen bond in structural chemistry and biology, Monographs on Crystallography, 9 (2001)1-526.
19. Boddohi S: Engineering Nano assemblies of polysaccharide, Advanced materials, 22 (2010) 2998-3016.
20. Stijnman A, Tromp R: Electrospinning of food–grade polysaccharide, Food Hydrocolloids, 25 (2011) 1393-1398.

21. Lee K, Jeong L, Kang Y, Lee S, Park W: Electrospinning of polysaccharide for regenerative medicine, Advanced Drug Delivery Reviews, 61 (2009) 1020-1032.

22. Manandhar S, Vidhate S, Souza N: Water soluble levan polysaccharide biopolymer electrospun fibers, Carbohydrate Polymers,78 (2009) 794-798.

23. Manasco JL, Tang C, Khan SA: Cyclodextrin fibers via polymer–free electrospinning, RSC Advances, 2 (2012) 3778-3784.

24. Uyar T, Celebioglu A: Electrospinning of Polymer–free Nanofibres from Cyclodextrin Inclusion Complexes, Langmuir, 27 (2011) 6218-6226.

25. Uyar T, and Kayaci F: Solid Inclusion Complexes of Vanillin with Cyclodextrin; Their Formation, Characterization, and High–Temperature Stability, Journal of agricultural and food chemistry, 59 (2011) 11772-11778.

26. Uyar T, Celebioglu A: Cyclodextrin nanofibres by electrospinning, Chem. Commun., 46 (2010) 6903-6905.

27. Rossi B, Gomez L, Fioretto D, Caponi S, Rossi F: Hydrogen bonding dynamics of cyclodextrin–water solutions by depolarized light scattering, J. Raman Spectroscopy, 42 (2011) 1479-1483.

28. Madhurima J, Sanjoy B: Vibrational spectrum of water confined in and around cyclodextrin, Chemical Physics Letters, 509 (2011) 181-185.

29. Charalampopoulos V, Papaioannou J: Dipole relaxation and proton transport in polycrystalline γ–cyclodextrin hydrate; A dielectric spectroscopy study, Solid State Ionics, 191 (2011) 1-11.

30. Challa R, Ahuja A, Ali J, Khar R: Cyclodextrin in drug delivery; An updated review, AAPS Pharm Sci Tech., 6 (2005) 329-357.

31. Lepe P, Tucker N, Simmons L, Watson A, Fairbanks A, Staiger M: Sub-micron sized saccharide fibres via electrospinning, De Gruyter Open – Electrospinning, 1 (2016) 1–9.

32. Poland D, Scheraga H: Energy Parameters in Polypeptides I; Charge distributions and the hydrogen bond, Biochemistry, 6 (1967) 3791-3800.

33. Yan J, Momany F, Hoffmann, Scheraga H: Energy Parameters in Polypeptides II; Semi empirical Molecular Orbital Calculations for model peptides, Physical chemistry, 74 (1970) 420-433.

34. Yan J, Momany F, Hoffmann H, Scheraga H; Energy Parameters in Polypeptides III; Semi empirical Molecular Orbital Calculations for Hydrogen–Bonded Model Peptides, Physical Chemistry, 74 (1970) 2424-2438.

35. Akira H: Supramolecular Polymer Chemistry, Wiley–VCH, (2011) 1-361.

36. Onsager L. Electrostatic interaction of molecules, Journal of Physical Chemistry, 43 (1939) 189-196.

37. Wan Y, He J, Yu J: Allometric scaling and instability in electrospinning, International journal of nonlinear sciences and numerical simulations, 5 (2004) 243-252.

38. Van Honschoten J, Tas N, Brunets N: Capillarity at the nanoscale, Chemical society reviews, 39 (2009) 1096-1114.

39. Wautelet M: Scaling laws in the macro, micro and nanoworlds, Institute of Physics Publishing, 22 (2001) 601-611.

40. Israelachvili J: Intermolecular and Surface Forces, Elsevier –Academic Press, 3 (2011) 1-674.

41. Shenoy S, Bates W, Wnek G: Correlations between electrospinnability and physical gelation, Polymer, 46 (2005) 8990-9004.

42. McKinley G: Iterated stretching, extensional rheology and formation of beads–on–a–string structures in polymer solutions, Journal of Non–Newtonian Fluid Mechanics, (2006) 137-148.

43. Doyle P, McKinley G, Spiegelberg S: Relaxation of dilute polymer solutions following extensional flow, Journal of Non–Newtonian Fluid Mechanics, 76 (1997) 79-110.

44. Tirtaatmadja V: Drop formation and breakup of low viscosity elastic fluids; Effects of molecular weight and concentration, Physics of fluids, 18 (2006) 1-7.

45. Hiemenz P: Polymer chemistry; the basic concepts, CRC Press, 1 (1984) 1-738.

46. Fujita H: Polymer solutions, Studies on polymer science, Elsevier, Amsterdam, Netherlands, 9 (1990) 1-370.

47. Terakota I: Polymer solutions; An introduction to physical properties, John Wiley & Sons, 1 (2002) 1-349.

48. Freire J: Relaxation of flexible chains in dilute and non–dilute systems, Dynamic Monte Carlo results for linear and star chains, Macromolecules, theory simulations, 8 (1999) 321-327.

49. Rubistein M, Semenov A: Dynamics of Entangled solutions for associating polymers, Macromolecules, 34 (2001) 1058-1068.

50. Genotelle J, Mathlouthi M: Role of water in sucrose crystallisation, Carbohydrate polymers, 37 (1998) 335-342.

51. Quintas M, Brandao T, Silva C, Cunha R: Rheology of supersaturated sucrose solutions, Journal of Food Engineering, 77 (2006) 844–852.

52. Myers D: Surfaces, Interfaces and Colloids; Principles and Applications, Wiley-VCH, 2 (1999) 1-528.

53. Ninham W, Lo Nostro P: Molecular forces and self–assembly; in colloid, nano sciences and biology, Cambridge University Press, (2010) 1-360.

54. Gupta P, Elkins C, Long T, Wilkes G: Electrospinning of linear homopolymers of poly (methyl methacrylate); exploring relationships between fiber formation, viscosity, molecular weight and concentration in a good solvent, Polymer, 46 (2005) 4799-4810.

55. Arunan E: Categorizing hydrogen bonding and other intermolecular interactions, Pure Applied Chemistry –IUPAC recommendation, (2011) 1-5.

56. Desiraju G, Steiner T: The weak hydrogen bond in structural chemistry and biology, Journal of Crystallography, 123 (2001) 191-192.

57. Luzar A: Resolving the hydrogen bond dynamics conundrum, Journal of chemical physics, 113, (2000) 10663-10675.

58. Boltachev G, Baidakov V: Extended version of the Van der Waals capillarity theory, Journal of Chemical Physics, 121 (2004) 8594-8601.